Transactions, **SMiRT-26**
Berlin/Potsdam, Germany, July 10-15, 2022
Division II

AN EXPERIMENTAL AND NUMERICAL APPROACH OF THE FAILURE BEHAVIOUR OF CRACK FIELDS UNDER DIFFERENT TEMPERATURES

Stefan Weihe[1], Ludwig Stumpfrock[2], Ulrich Weber[1], Tim Schopf[1], Patrick Gauder[3], Michael Seidenfuss[4]

[1] Materials Testing Institute (MPA) University of Stuttgart, Stuttgart, Germany
[2] Materials Testing Institute (MPA) University of Stuttgart, Stuttgart, Germany (formerly)
[3] Institute for Materials Testing, Materials Science and Strength of Materials (IMWF) University of Stuttgart, Stuttgart, Germany (formerly)
[4] Institute for Materials Testing, Materials Science and Strength of Materials (IMWF) University of Stuttgart, Stuttgart, Germany

ABSTRACT

Crack tips of crack fields in the base material of pressure vessels undergo predominantly mixed-mode loading conditions under internal pressure, when the orientations of these fields are laminar or quasi-laminar to the pressure retaining surface. Furthermore, the induced stress and strain fields of the single crack tips influence each other. Indications of a high quantity of cracks from non-destructive testing measurements were determined in a root cause analysis as hydrogen flakes positioned in segregated zones in the base material of pressure vessels of Belgian nuclear power plants. In this paper, experimental results from notched tensile specimens, CTS-specimens and tensile specimens containing multiple flaws are presented. Additionally numerical simulations are carried out with an extended micromechanical based damage mechanics model. For the description of ductile failure mode the Rousselier model is used. To simulate the sensitivity for low stress triaxiality damage by shear loading, the damage mechanics model was enhanced with a term to account for damage evolution by shear. In this paper, the current state of the ongoing research project is presented.
Keywords: Rousselier, integrity, damage, mixed-mode

INTRODUCTION

A large number of crack-like findings in the ferritic wall were detected during routine ultrasonic investigations of the reactor pressure vessels (RPV) in the Belgian nuclear power plants Doel 3 and Tihange 2 in 2012. Further investigations and a root cause analysis lead to the conclusion that the indications are hydrogen flakes, which arose during the production of the RPV. The hydrogen flakes are located within segregation lines with an inclination of 0° (laminar) to 16° (quasi-laminar) to the pressure-retaining surface. The size of the hydrogen flakes vary from a few millimeters to several centimeters [Doel 3 (2012), Tihange 2 (2012)].

For the safety-related integrity assessment of pressurized components with multiple flaws, standards and guidelines are using interaction criteria and substitution procedures for the evaluation of multiple flaws [FKM (2009), ASME (2015), ASME (2016)]. These interaction criteria are based on linear-elastic fracture mechanic and experiments based on pure mode I [Hasegawa et al. (2009), Lacroix et al. (2015)].

The aim of the presented research work is to develop interaction criteria based on a damage mechanical approach. Damage mechanics allow predicting the local plastic deformation as well as the

failure mechanisms for any given geometry from the stress and strain state [Beremin (1983), Rousselier (1987), Seidenfuß et al. (2014)]. The investigated failure mechanisms are stable crack initiation and stable crack growth as well as cleavage fracture probability. These failure mechanisms can occur in the ductile-to-brittle transition region of material toughness. The investigation of this region is important, because of the embrittlement of material due to radiation, aging or low temperatures [Schuler et al. (2015)].

In this paper a material characterization is done with notched round bars and shear (CTS) specimens to investigate the influence of temperature and different stress states on the damage behavior. Furthermore, tensile specimen with artificial crack fields are manufactured and tested.

EXPERIMENTAL RESULTS

In the current phase the experimental investigations are expanded to a wide temperature field from room temperature (RT ≈ 20°C) till T = -180°C to investigate the influence of the stress triaxiality on the lower shelf temperature of the ferritic low alloy steel 22NiMoCr3-7.

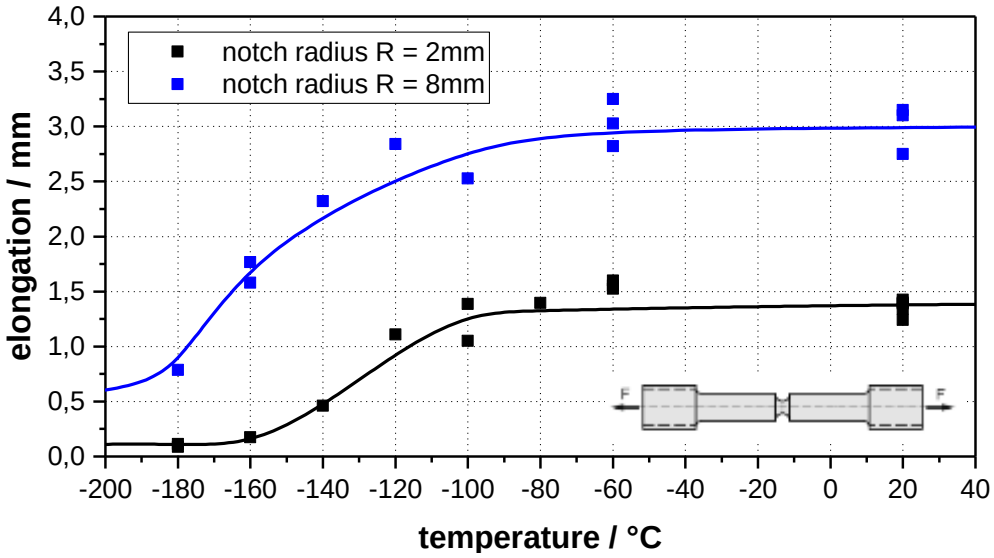

Figure 1. Elongation till failure vs temperature for notched tensile specimen with notch radius R = 2mm and R = 8mm.

In Figure 1 the elongation of notched tensile specimen till failure vs temperature is shown for two notch radii R = 2mm and R = 8mm. Besides the lower ductility of the specimen with R = 2mm (less elongation) the lower shelf temperature of the sharper notched specimen is in the range of T = -160°C and

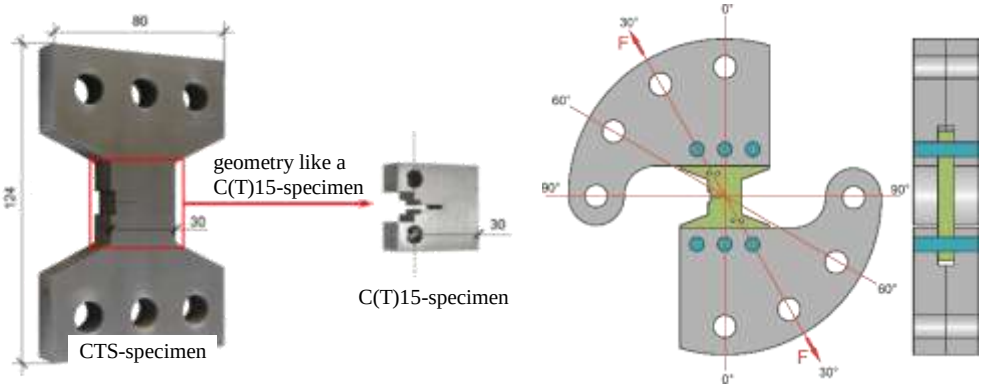

Figure 2. Schematic of a CTS-specimen and its clamping

is higher then the temperature of the notched specimen with R = 8mm. Besides the tensile test, so called Compact Tensile Shear (CTS) specimens are tested [Richard et al. (2013)], to investigate the material behavior for mode II and two mixed-mode loadings (30° and 60°). The CTS specimen is based on a Compact Tension (C(T)15-) specimen with a fatigue pre-crack. To realize the different loading angles a special clamping is used, see Figure 2. These CTS-specimens under mixed-mode loading were tested at different temperatures to determine the temperature between ductile and brittle failure, see Figure 3.

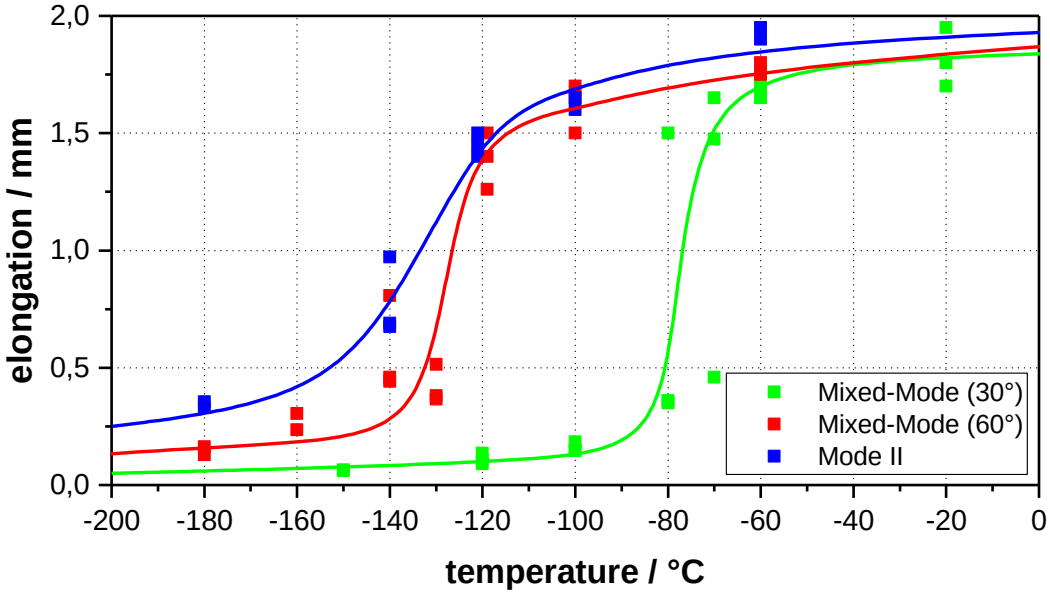

Figure 3. Elongation till failure and till maximum load vs temperature for CTS specimens under pure mode II and mixed-mode loading.

Also for CTS specimens the lower shelf temperature of the material depends on the stress state due to the loading angle. For a mixed-mode loading under 30°, the lower shelf temperature is in the range of T = -120°C whereas for mixed-mode loading under 60° the temperature is around T = -160°C. For CTS-specimen under pure mode II, the lower shelf temperature is below T = -180°C, because ductile regions in the range of 50µm are observed on the crack surface, see Figure 4 (SEM = Scanning Electron Microscope).

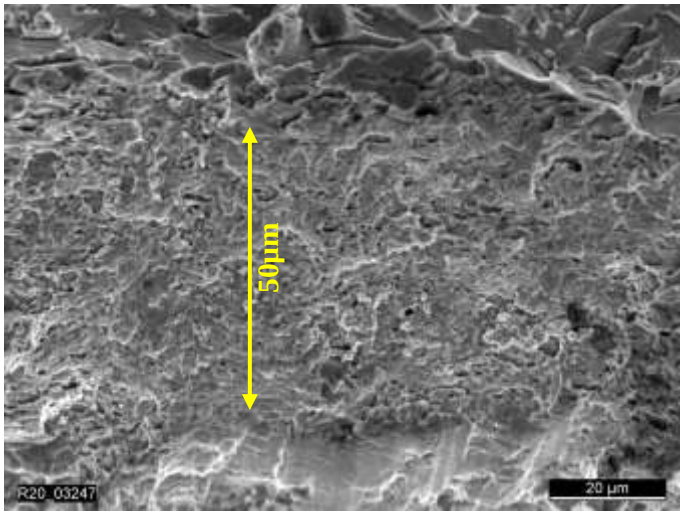

Figure 4. CTS-specimen under pure mode II tested at T = -180°C: SEM image of the fracture surface with ductile region.

Besides the material characterization of the material 22NiMoCr3-7, experiments are carried out to investigate the failure behavior of specimens with artificial crack fields. In Figure 5 an artificial crack field specimens is shown. The artificial trough-thickness cracks are eroded in the middle of the specimens and have a crack tip radius of 0.15mm.

Figure 5. Typical specimen for the investigation of artificial crack fields from 22NiMoCr3-7.

Lacroix et al. (2015) derive interaction rules for quasi-laminar flaws. This work is based on 2D eXtended Finite Element Method (X-FEM) calculations. From this calculations, the following proximity rules are defined as: Two quasi-laminar flaws shall be grouped (or interact) if the threshold parameters k_h = H/D and k_s = S_1/D reaches the values given in Table 1 (an additional margin of 20% is considered to determine the threshold parameters k_h and k_s). The interaction curves are shown in Figure 6. In the regions outside the curves, no crack interactions are assumed.

Table 1: Comparison of interaction criteria threshold between 2D and 3D cases (H = horizontal distance of the flaw tips, S_1 = vertical distance of the flaw tips, D = half flaw size).

	Elliptical flaw (3D)	Infinite flaw (2D)
Alignment criterion threshold k_h = H/D	0.34	0.85
Combination criteria threshold k_s = S_1/D	0.73	2

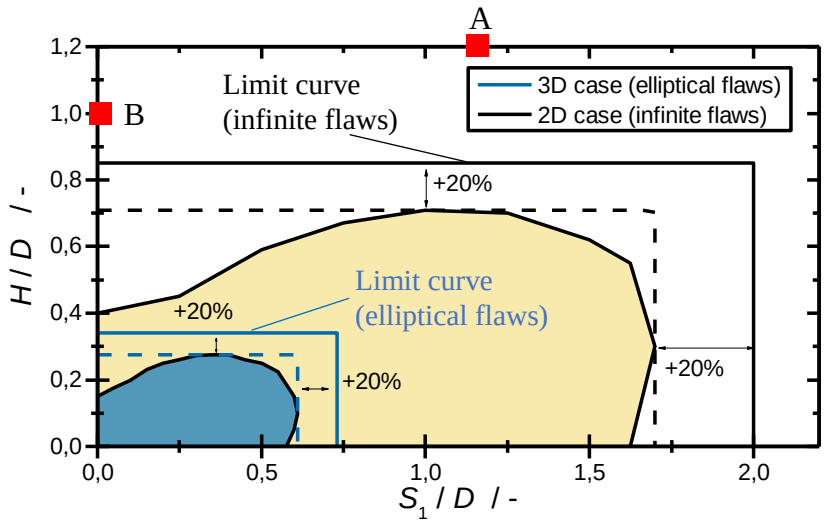

Figure 6. Interaction curves and associated interaction criteria: Comparison between 2D and 3D. A and B are the investigated flaw configurations (Lacroix et al. (2015)).

In this paper, two kinds of flaw configurations are investigated (Figure 7). In flaw configuration A, both, the horizontal and the vertical distance of the flaw tips are 4.5mm with a flaw size of 7.5mm. The H/D ratio and the S_1/D ratio is each 1.2. In flaw configuration B, the vertical distance S_1 of the flaw tips is zero and the horizontal distance H is 3.75mm which leads to a ratio H/D = 1 and S_1/D = 0. Both flaw configurations are marked in Figure 6.

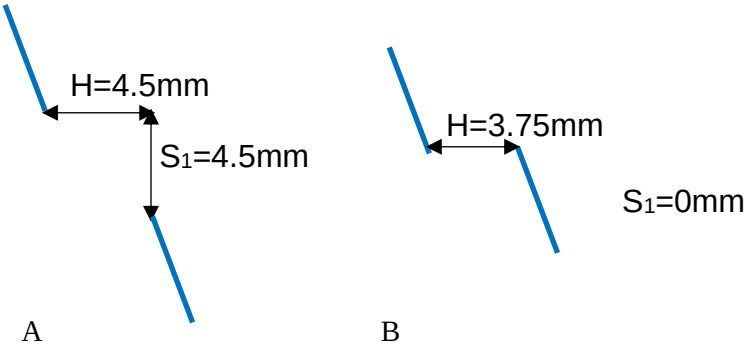

Figure 7. Flaw configuration A with H/D = S_1/D = 1.2 and flaw configuration B with H/D = 1 and S_1/D=0. Half flaw size and flaw angle are D = 3.75mm and α = 20°, respectively.

As can be seen in Figure 6, the distance between the interaction curve (2D case curve (infinite flaws)) and flaw configuration A is quite larger than the distance of configuration B. In both cases it is expected, that the flaw tips do not interact and must not be grouped, respectively. Both flaw configurations are tested at T = -60°C and T = -100°C. Figure 8 shows the fractured specimen. As expected from the interaction curve there is no interaction of the flaw tips for flaw configuration A for both temperatures T = -60°C and T = -100°C. However, the flaw tips in configuration B interact for both temperatures, which is in contrast to the interaction curve given in Figure 6.

Figure 8. Fractured flaw field specimen; A1: Flaw configuration A at T = -60°C ; A2: Flaw configuration A at T= -100°C ; B1: Flaw configuration B at T = -60°C ; B2: Flaw configuration B at T = -100°C.

NUMERICAL RESULTS

Numerical simulations are carried out with extended micromechanical based damage mechanics models. For the description of ductile failure mode the Rousselier model is used (Rousselier et al. (1987)).
The original Rousselier model shows good results for high and intermediate stress triaxiality. To predict shear failure with low stress triaxiality the Rousselier model is extended with an additional term (Gauder et al. (2020)). A detailed description of the extended model is given in Fehringer et al. (2018).

Figure 9 shows the comparison between the experiment and the simulation for flaw configuration A (left) and flaw configuration B (right) for both temperatures T = -60°C and T = -100°C. Except flaw configuration B at T = -60°C, where the simulation fails before the experiment, there is a good agreement between the numerical and the experimental results.

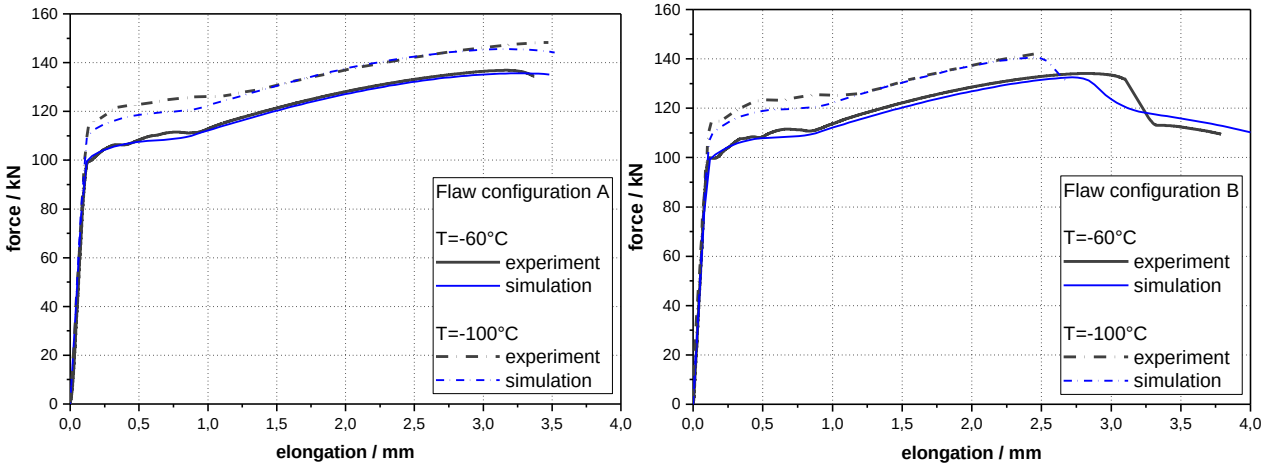

Figure 9. Force-elongation curves for flaw field configuration A (left) and flaw field configuration B (right): Experiment and simulation.

CONCLUSION AND OUTLOOK

As expected, the transition temperature and the lower shelf temperature depend strongly on the stress triaxiality. The less the stress triaxiality, the less is the transition temperature. Notched tensile specimen with notch radii of R = 2mm reach the lower shelf at T = -160°C where as the specimen with R = 8mm is still ductile al T = -180°C.

In the case the of mixed-mode loaded CTS specimens the temperature decreases from mixed-mode loading (30° over 60°) to mode II loading. For mode 30°, the lower shelf temperature is in the range of T = -120°C whereas for mode 60° the temperature is around T = -160°C. Under mode II the lower shelf temperature is below T = -180°C because the crack surface of this specimen, tested at T = -180°C shows ductile regions in the range of 50µm.

The experimental investigation of two kinds of flaw configurations shows, that the characterization rules for quasi-laminar flaws, which predicts no interaction of the flaws, are not valid for one investigated flaw configuration. The numerical simulations with the extended micromechanical based damage mechanics model show a good agreement with the experimental results.

For a better numerical description of the failure behaviour of specimens at low temperatures a combined damage model (mod. Rousselier - mod. Beremin) [Final Report (2019)] will be used in the ongoing research project.

ACKNOWLEDGEMENTS

This research work is funded in the framework of the German reactor safety research program by the Federal Ministry for Economic Affairs and Energy (BMWi) under contract No. 1501596A. The support is gratefully acknowledged.

Supported by:

Federal Ministry
for Economic Affairs
and Energy

on the basis of a decision
by the German Bundestag

REFERENCES

ASME Boiler & Pressure Vessel Code, Section XI (2015). "Rules for In-service Inspection of Nuclear Power Plant Components".

ASME BPVC.CC.NC-2017 Case N-848-1 (2016). "Alternative Characterization Rules for Quasi-Laminar Flaws".

Beremin: A. (1983). "Local Criterion for Cleavage Fracture of a Nuclear Pressure Vessel Steel," *Metallurgical Transactions A, No. 14A*, pp. 2277-2287.

Doel 3 Reactor Pressure Vessel Assessment, Safety Case Report, Electrabel GDF Suez, 5.12.2012.

Fehringer F., Schuler X., Seidenfuß M. (2018). „Development of a damage mechanics based limit strain concept using an enhanced Rousselier model," *ECF22 Structural Integrity Procedia*.

Final Report MPA Stuttgart (2019). "Experimental and numerical investigations on crack fields in pressurised components (MeKom)", Subproject: "Micromechanical modeling of systematic crack fields and formation of an assessment criterion," Reactor Safety Research – Project No. 1501513A.

Forschungskuratorium Maschinenbau e.V. (FKM 2009). „Bruchmechanischer Festigkeitsnachweis für Maschinenbauteile", 3. Auflage, VDMA Verlag, GmbH.

Gauder, P.; Seidenfuß, M.; Stumpfrock, L. (2020). „Experimentelle und numerische Untersuchungen zu Mehrfachrissen in Komponenten der druckführenden Umschließung (MeKom)," *Final Report; MPA Universität Stuttgart*, Stuttgart.

Hasegawa, K., Koichi, S., Katsumasa, M. (2009). „Alignment Rule for Non-Aligned Flaws for Fitness-for-Service Evaluations Based on LEFM," *Journal of Pressure Vessel Technology, Vol. 131*.

Lacroix, V., Dulieu, P., Bogaert, A. (2015). „Alternative characterization rules for quasi-laminar flaws based on 3D X-FEM calculations," *Proceedings of ASME Pressure Vessels & Piping conference (PVP 2015)*, PVP2015-45792, Boston, USA.

Richard, H. A.; Schirmeisen, N.-H.; Eberlein, A. (2013). „Experimental investigations on mixed-mode-loaded cracks;" *Proceedings of the 4th International Conference on crack paths*, pp. 219-233

Rousselier, G. (1987). "Ductile Fracture Models and their Potential in Local Approach of Fracture," *Nuclear Engineering and Design, Volume 105*, pp. 97-111.

Schuler. X., Seidenfuß M. (2015). „Experimentelle und numerische Untersuchungen zu Mehrfachrissen in Komponenten der druckführenden Umschließung (MeKom)," BMWi- Joint Research Project.

Seidenfuß, M. (2014). „Schädigungsmechanische Modelle zur Beschreibung des Versagensablaufs in metallischen Bauteilen," *Technical Report, MPA University of Stuttgart*.

Tihange 2 Reactor Pressure Vessel Assessment, Safety Case Report, Electrabel GDF Suez, 5.12.2012.